CrossMark

Improving the integrity and the microstructural features of electron beam welds of a creep-resistant martensitic steel by local (de-)alloying

Antonia Rabl[1] · Florian Pixner[1] · Bruno Duarte[1,2] · Danijel Blatesic[1] · Coline Béal[1] · Norbert Enzinger[1]

Abstract

Martensitic 9–12% chromium steels present the most preferred material group for high-temperature components in thermal power plants. Previous investigations revealed that due to the use of a creep-resistant martensitic steel strengthened with boron and nitrogen (MarBN), the minimum creep rate can significantly be decreased. Furthermore, the formation of the fine-grained heat-affected zone (FGHAZ) due to welding can be suppressed. This FGHAZ is subject to the most dominant failure mode (type IV cracking) of welded joints during creep exposure. By using electron beam welding, the total width of the heat-affected zone (HAZ) can be reduced compared to conventional arc welding processes. Preceding investigation on electron beam welding of MarBN steel showed recurring difficulties with hot cracking within the fusion zone. Various approaches were tried to produce defect-free welds without the use of any filler metal, but no satisfactory results were achieved. In this investigation, the chemical composition of the fusion zone was modified by the addition of conventional 9% chromium creep-resistant steel as a filler material. By using the filler material, the fusion zone was locally (de-)alloyed and defect-free joints of MarBN steel were produced.

Keywords MarBN steel · 9–12% Cr steels · EBW · Focus wobbling · Welding of large cross sections · Local (de-)alloying

1 Introduction

To improve the efficiency of thermal power plants, the steam temperature and inlet pressure of turbines have to be raised. These demands coming from the power-generating industry entail challenges to materials science and welding technology because increasing steam temperatures require the use of materials with improved creep and oxidation resistance during long-term service [1–3].

Martensitic 9–12% chromium steels strengthened by controlled addition of boron and nitrogen (MarBN) especially were developed for operating temperatures up to 650 °C.

Due to dissolved B, which acts as a solid solution strengthener and $M_{23}C_6$ precipitate stabilizer, the coarsening rate of

$M_{23}C_6$ precipitates during creep is reduced and so the onset of acceleration creep is retarded [4]. Finely distributed MX carbonitrides rich in vanadium/niobium are responsible for a precipitation strengthening [5].

The microstructural changes which result from the thermal input of the joining process are prone to premature cracking during service conditions. The most dominant failure mode is categorized as type IV cracking and it occurs in the fine-grained heat-affected zone (FGHAZ) of welded joints [3]. Due to controlled addition of boron and nitrogen, the formation of the FGHAZ can be suppressed. However, some fine grains along the prior austenite grain boundaries (PAGB) in the heat-affected zone (HAZ) can still be found [6].

For these investigations, the electron beam welding (EBW) process was used for joining the MarBN steel NPM1-P. The welding process is characterized by a high energy density (~ 10^7 W cm^{-2}) and high welding speeds. The high power density of the process vaporizes the material instantly, generating a vapor capillary. With this so-called keyhole technique, it is possible to join very thick cross sections in one single layer without the use of any filler material. Furthermore, it is possible to produce deep and narrow welds with a very thin HAZ. Nonetheless, due to the high welding speed, the solidification

✉ Antonia Rabl
antonia.rabl@tugraz.at

1 Graz University of Technology, Institute of Materials Science, Joining and Forming, Kopernikusgasse 24, 8010 Graz, Austria

2 Present address: Faculdade de Ciências e Tecnologia da Universidade Nova de Lisboa, Calçada de Alfazina 2, 2825-149 Caparica, Portugal

process is very fast which results in a fine microstructure in the fusion zone [7, 8].

Preceding investigations of the EB-welded MarBN steel showed a recurring problem of hot cracking in the fusion zone. Within this study, the appearance of the welding defects is called "microfissure" because of the small size of the defects. The formation mechanism, however, resembles hot cracking. A Design of Experiments (DoE) was conducted to investigate the influence of varying parameters (accelerating voltage, beam current, welding speed, and beam figure) on the welding result. By using a dynamic lens in the EBW device, the so-called focus wobbling technique, it was possible to reduce the accumulated number and length of the occurring microfissures; nonetheless, it was not possible to completely suppress them [9].

In order to prevent the formation of microfissures within the fusion zone, the new focus was placed on influencing the chemical composition of the joints and the behavior during solidification by the use of a filler material [10–12]. In this study, the filler material was placed like a sheet between the joining parts. The selection of a filler material and the minimum required dilution for an integer joint is investigated.

2 Experimental procedure

2.1 Materials

For all welding experiments performed within this contribution, the forged NPM1-P steel was used. Following the approach of Japanese scientists of the National Institute for Materials Science (NIMS), this type of steel has been designed by the Institute of Materials Science, Joining and Forming (IMAT) of Graz University of Technology [13]. The chemical composition of the base material is given in Table 1.

Prior to welding, the base material was subjected to a quality heat treatment to achieve a tempered martensitic structure with $M_{23}C_6$ and MX precipitates which are responsible for the good creep properties [14]. The standard quality heat treatment consists of normalizing at 1120 °C for 1 h, air cooling, followed by two times tempering at 750 °C for 3 h each and subsequent air cooling [15].

Preliminary investigations revealed a serious hot cracking problem of the NPM1 steel; therefore, the hot crack susceptibility of two conventional martensitic 9% Cr creep–resistant steels (P91, P92) was investigated. Their major alloying elements are shown in Tables 2 and 3.

All three 9% chromium base materials show very similar chemical compositions. However, unlike P92 and NPM1, P91 does not contain boron, cobalt, and tungsten. P92 was developed by improving the creep rupture strength of P91 steel in order to achieve higher steam temperatures and inlet pressures of power plants [17]. The improvement of the creep strength was obtained by alloying small amounts of boron. As a consequence, fine $M_{23}C_6$ carbides near prior austenite grain boundaries (PAGB) are stabilized, and so the onset of acceleration creep is retarded [5, 18, 19].

Since boron is believed to be promoting hot cracking in the fusion zone, the influence of boron (and nitrogen) on the hot crack susceptibility of the MarBN steel was investigated by modifying the chemical composition by local (de-)alloying.

2.2 Welding

For the welding experiments, the pro-beam EBG 45-150 K14 electron beam welding (EBW) device of the Institute of Materials Science, Joining and Forming (IMAT) at Graz University of Technology was used. This highly innovative power machine is equipped with a 150-kV-45-kW generator. All experiments were conducted in flat welding position (PA) with an optimized parameter configuration (Table 4) which was determined in preceding experiments. Because of the recurring hot cracking problem of the MarBN steel NPM1, comparative beads on plate welds (blind welds) with P91 and P92 steels were performed using the optimized parameter configuration with the dynamic lens. This procedure is characterized by an oscillation of the beam over the thickness of the workpiece. For all experiments, the welding parameters were kept constant.

Non-destructive testing as well as metallography and microscopy investigations of the P91 welds showed no microfissures within the fusion zone. However, the investigated cross sections of P92 revealed lateral and transversal microfissures in the fusion zone; concluding, P91 is less susceptible to hot cracking than P92. Based on this knowledge, subsequent welding investigations were performed between NPM1 and P91.

The first approach to modify the chemical composition of the weld metal was to progressively add P91 to the NPM1. Therefore, the joint preparation of the welding samples was in that way, that the abutting face of the joining parts had an inclination angle α of 1°. The electron beam, however, followed the dashed, horizontal line (Fig. 1a).

Table 1 Chemical composition of the MarBN steel NPM1-P in wt.%

	C	Mn	Cr	Mo	Co	W	V	Nb	N	B	Fe
[wt.%]	0.07	0.5	9.0	0.05	2.9	2.9	0.2	0.05	0.01	0.01	Bal.

Table 2 Major alloying elements of P91 in wt.% [16]

[wt.%]	C	Mn	Cr	Mo	Co	W	V	Nb	N	B	Fe
Min.	0.08	0.30	8.0	0.85	–	–	0.18	0.06	0.03	–	Bal.
Max.	0.12	0.60	9.5	1.05	–	–	0.25	0.10	0.07	–	

Table 3 Major alloying elements of P92 in wt.% [16]

[wt.%]	C	Mn	Cr	Mo	Co	W	V	Nb	N	B	Fe
Min.	0.07	0.30	8.5	0.30	–	1.5	0.15	0.04	0.03	0.001	Bal.
Max.	0.13	0.60	9.5	0.60	–	2.0	0.25	0.09	0.07	0.006	

Caused by this setup and the constant parameters during the welding process, the weld metal is constituted by a variable dilution of both materials. Different positions of the weld seam were investigated and, depending on the investigated position, different dilutions were determined. These first welding trials showed that with an increasing amount of P91, the hot cracking resistance improved significantly.

Based on these findings, the second approach to obtain a modification of the chemical composition was to use P91 as a filler material. This was done by placing thin sheets (interlayers) of P91 between two blocks of NPM1 (Fig. 1b), which then were joined using the constant parameter configuration. Because of the influence of the dilution of the involved materials, joint welds with three different interlayer thicknesses were produced to ensure crack-free welds, each thickness (1.5 mm, 2.0 mm, and 2.5 mm) being representative for a certain dilution.

2.3 Characterization

For the characterization of the interlayer welds, samples were prepared for microstructure and hardness investigations by using standard metallographic techniques. The microstructural examinations were conducted using light optical microscopy (LOM) and scanning electron microscopy (SEM).

Furthermore, hardness measurements according to EN ISO 6507-1:2016 were performed using an EMCO TEST M1C 010 with a load of 1 kg and a dwell time of 15 s.

Table 4 Optimized parameter configuration which was used for all welding experiments

Beam current I	150 mA
Acceleration voltage U	120 kV
Welding speed u	8.0 mm/s
Energy input E	22.5 kJ/cm
Beam figure	Circle
Beam diameter	0.5 mm
Working distance	800 mm
Focus wobbling	
Focal point	− 40 mm
Wobbling amplitude (in Z direction)	2550 mA/15 mm
Frequency	500 Hz

3 Results and discussion

3.1 Microstructure

Microstructural analysis of the weld metal resulting from the interlayer welds was conducted by using light optical microscopy. Detailed micrographs of the etched samples show a tempered martensitic microstructure in the base metal (Fig. 2a) as a result of the quality heat treatment prior to the welding process. Within the fusion zone and along the weld interface, bright appearing regions were found (Fig. 2b). These regions can be assigned to delta ferrite, which is formed during the welding process [20].

Pursuing scanning electron microscopy (SEM) investigations were carried out with respect to the occurrence of welding defects. Figure 3a shows the macrograph of a cross section of the 1.5-mm interlayer weld, which correlates with a dilution of approximately 60% P91 and 40% NPM1. Several welding defects were found in the fusion zone and SEM investigations revealed obvious microfissures and pores within the fusion zone.

The cross sections with the interlayer thickness of 2.0 mm (approx. 80% P91 and 20% NPM1) showed no microfissures macroscopically (Fig. 3b). SEM investigations of the embedded cross section showed some pores and lack of fusion between interlayer and base metal.

However, investigations of the cross sections welded with the 2.5-mm-thick interlayer showed a massive lack of fusion. The lack of fusion is due to the width of the interlayer, which, due to the constant parameters, was wider than the width of the weld seam.

Because of the satisfactory results of the 2.0mm interlayer—no microfissures were found within the fusion zone—EDX line scans were conducted on various positions of the cross section to guarantee a homogeneous mixture within the fusion zone of the involved martensitic steels (Fig. 4).

Despite the fact that the welds with an interlayer thickness of 2.0 mm showed macroscopically no hot crack formation, a bright appearing phase was found in the fusion zone under the light optical microscope (Fig. 5a). To characterize the formation, microhardness tests were conducted. Results of the hardness tests revealed a microhardness of nearly 860 HV, so it could be concluded that it was no delta ferrite. Therefore, EDX and electron backscatter diffraction (EBSD) investigations were conducted.

EDX line scan analysis indicated a slightly higher Cr content compared to the base material (Fig. 5b). Therefore, the bright color could be explained by a lower etching attack, respectively, and the found phase might have a higher corrosion protection.

Further SEM investigation and EDX spot scan analysis revealed higher concentration of molybdenum in some areas of the phase, and in addition, defects were detected in the
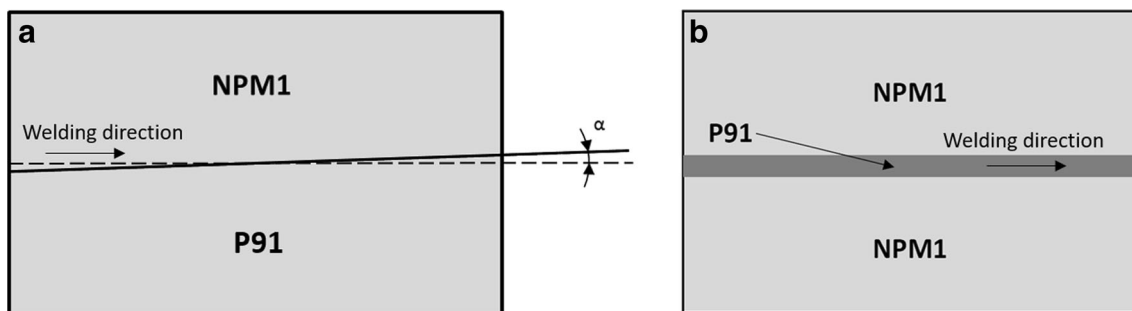
Fig. 1 Experimental setup for joint welds (**a**) with an inclination angle of 1° between the joining parts and (**b**) with a P91 interlayer

vicinity of the areas, causing the formation of cavities. The crystal structure, obtained by EBSD measurements, however indicated a $M_{23}C_6$ precipitate (Fig. 6).

3.2 Chemical composition of the cross sections

To verify the feasibility of local (de-)alloying, a chemical analysis of the cross sections of the interlayer welds with 1.5 mm and 2 mm was performed by optical emission spectroscopy. In addition, a reference joint weld of two NPM1 blocks without the use of any filler material was chemically analyzed. The results of the chemical analysis are shown in Table 5. On the basis of these quantitative values and considering the resolution of the measurement technique, a tendency can be recognized and the feasibility of local (de-)alloying was confirmed.

3.3 Hardness distribution

To investigate the hardness distributions across the weld seam of the interlayer welds, Vickers hardness measurements were conducted. Figure 7 shows the results of the hardness mapping of the 2.0mm interlayer weld compared with the hardness distribution of the two welded base materials.

All three hardness distributions have in common a high hardness in the weld metal and a slight hardness drop in the

transition zone between HAZ and fusion zone, which might be due to the formation of delta ferrite. The formation of delta ferrite during the welding process is mainly situated at the weld metal interface because of the epitaxial growth during the start of the solidification process [20, 21]. The high hardness within the fusion zone, compared to the base material, is due to the small grain size and the freshly formed martensite which is typical for electron beamwelded martensitic steels [22].

The NPM1 base material hardness is about 250 HV, whereas the P91 base material reaches values of about 230 HV. Within the fusion zone, the NPM1 also shows slightly higher hardness values (404 HV1) than the P91 (390 HV1). However, the hardness distribution of the 2.0mm interlayer weld is characterized by a hardness with maximum values of 440 HV1 in the fusion zone and 417 HV1 in the HAZ.

The reason for the overall higher hardness within the fusion zone of the interlayer welds has to be investigated more in detail.

4 Summary and conclusions

Previous investigations on the electron beam weldability of the MarBN steel NPM1-P showed a recurring problem of hot cracks within the fusion zone. To overcome
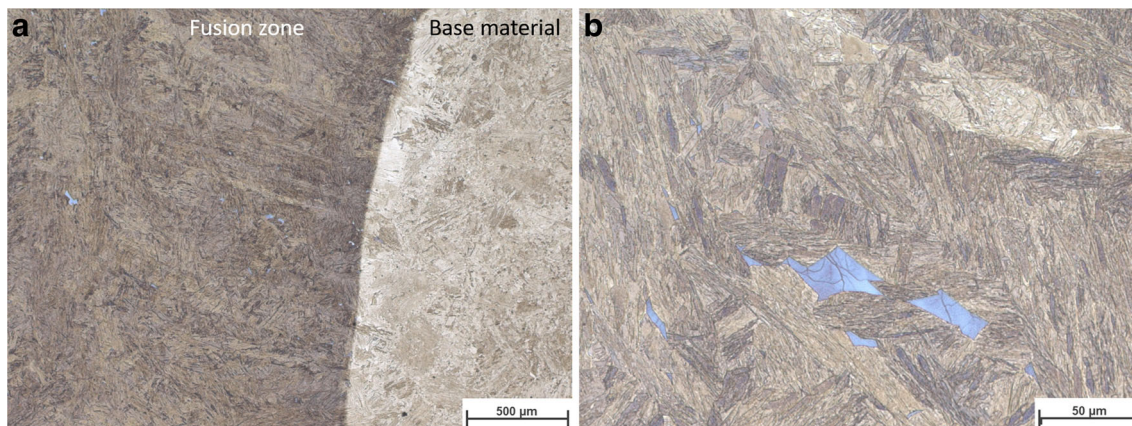

Fig. 2 **a** Transition from the fusion zone to the base material. **b** The microstructure of the fusion zone
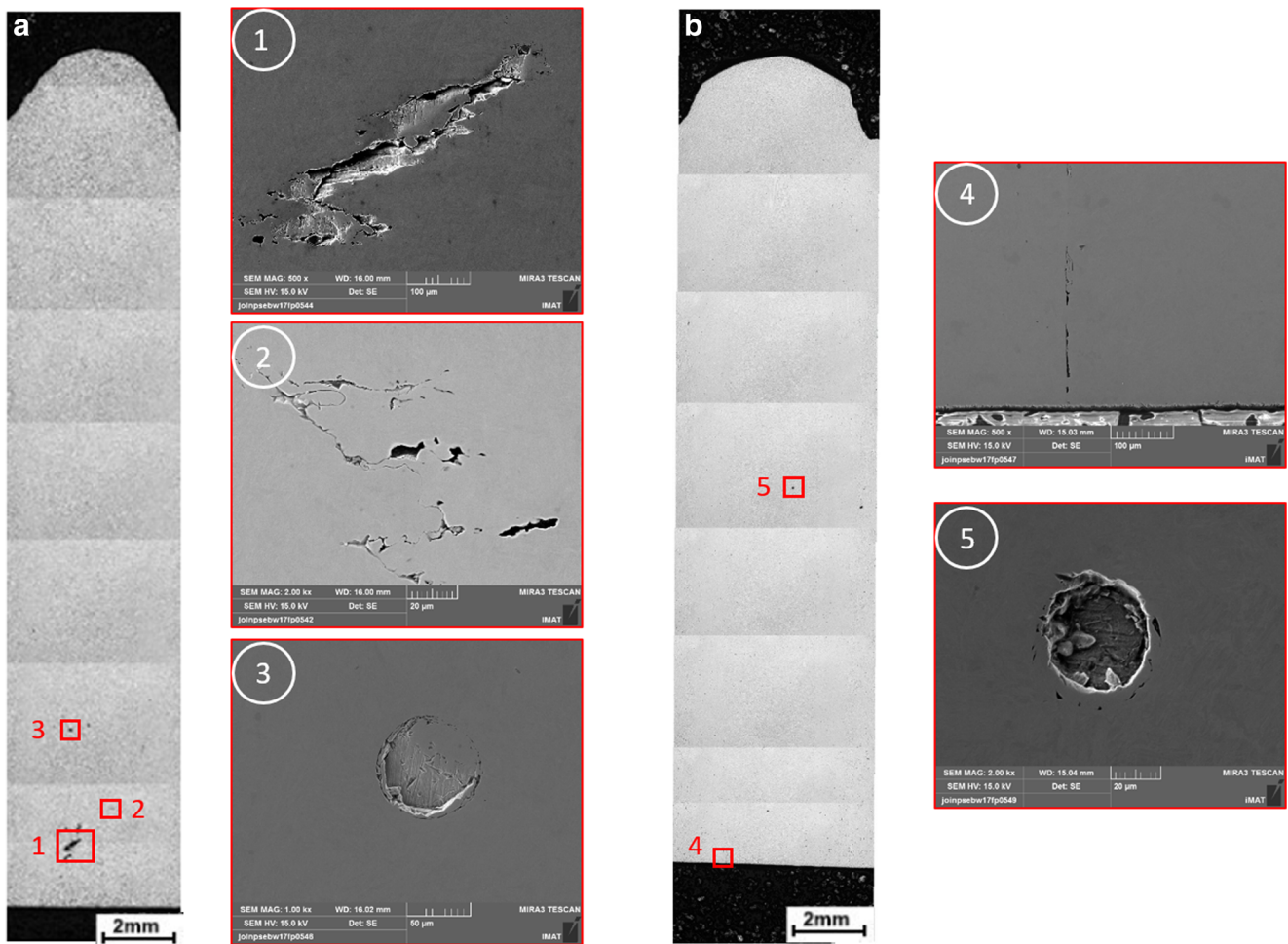
Fig. 3 Macrograph and SEM images of cross sections of interlayer welds with (a) thickness of 1.5 mm (60% P91) and (b) thickness of 2.0 mm (80% P91)

this problem, the approach of using a filler metal was conducted in this study. Therefore, welding studies with two conventional 9% Cr creep–resistant steels were carried out.
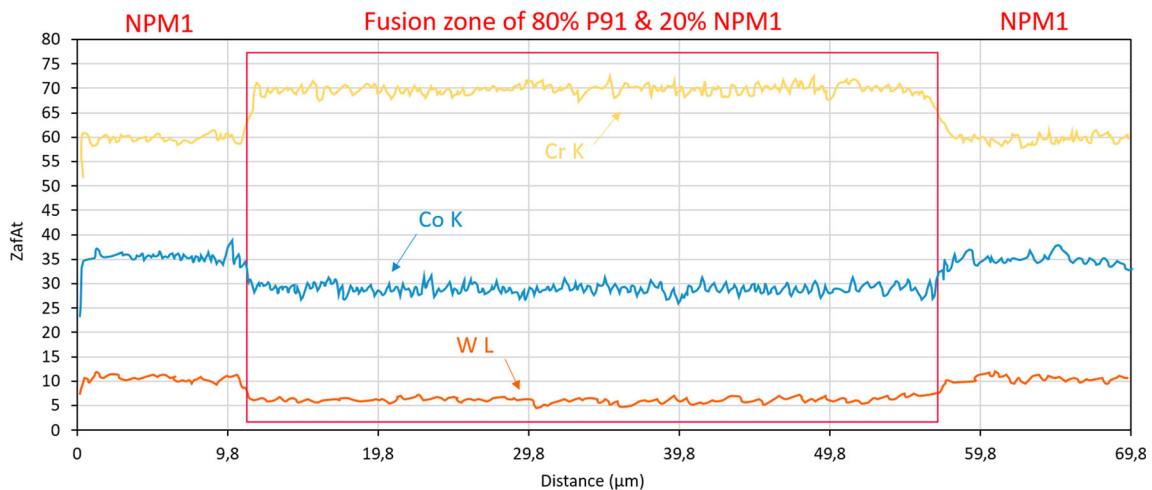
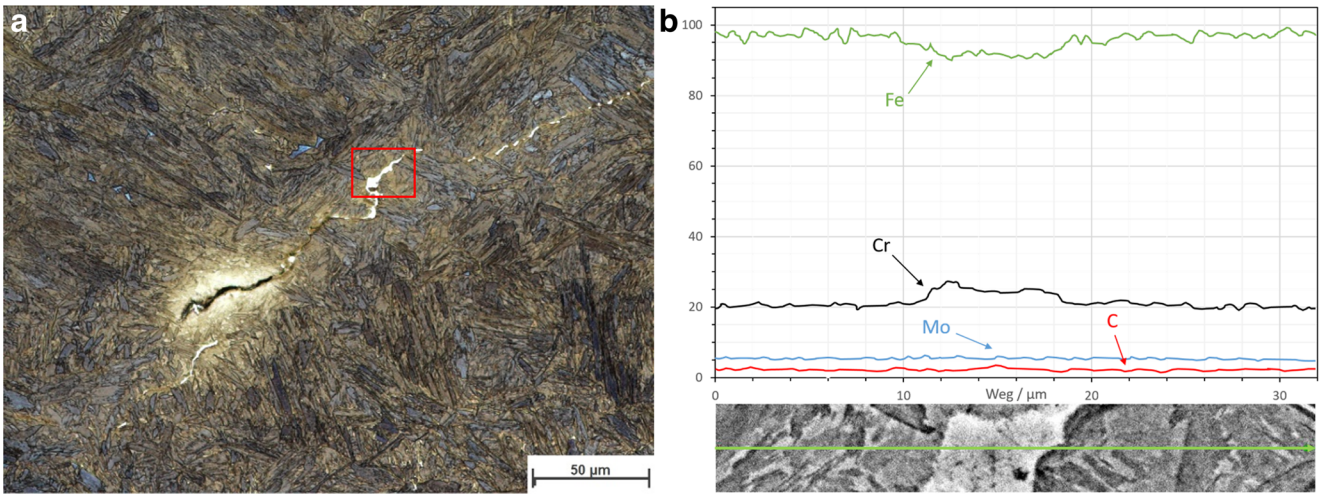Fig. 4 EDX line scan of the 2mm interlayer joint weld between NPM1 and P91 (fusion zone red boxed)

Fig. 5 **a** LOM picture of a bright phase in the fusion zone of an interlayer weld. **b** EDX line scan of the phase
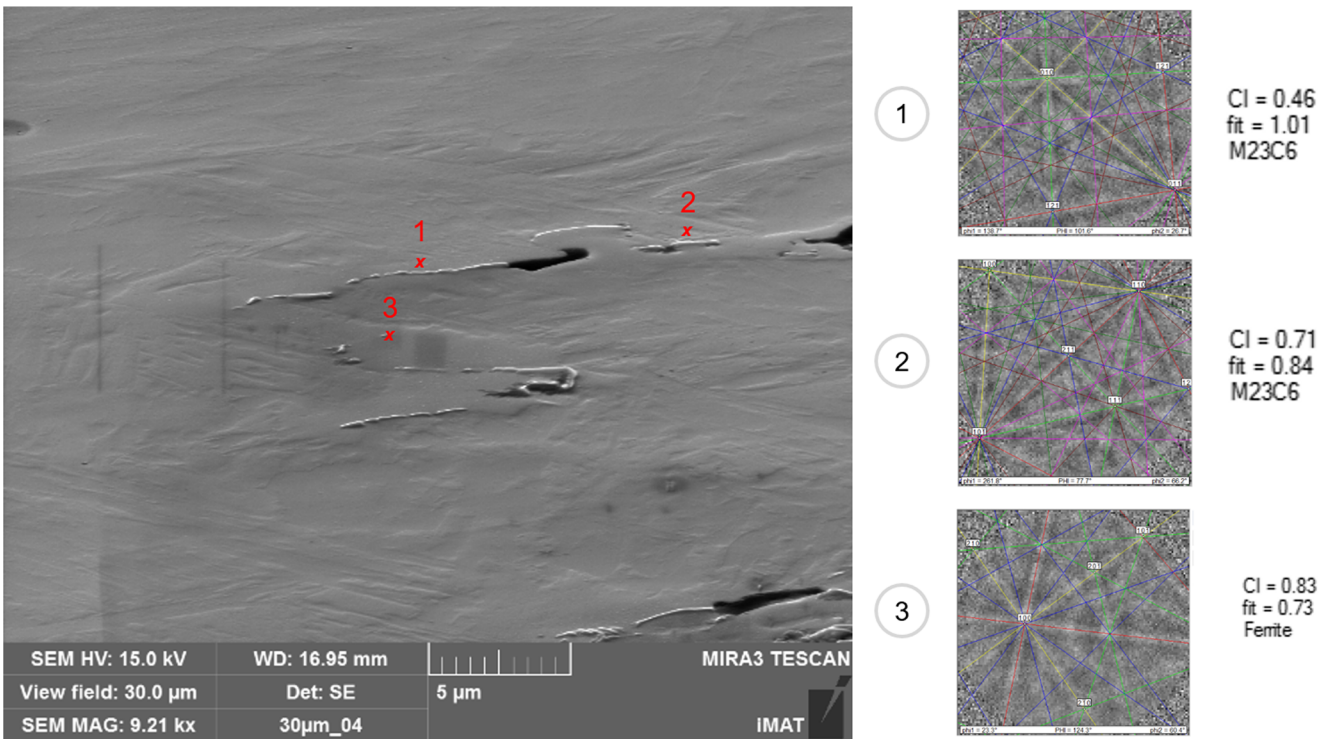

Fig. 6 EBSD investigation of three spots along the found phase (left) with corresponding Kikuchi patterns (right)

Table 5 Chemical composition of fusion zone after local (de-)alloying in wt.%

	C	Mn	Cr	Mo	Co	W	V	Nb	N	B	Fe
1.5 mm	0.112	0.443	9.12	0.783	0.492	0.453	0.207	0.069	0.042	0.001	Bal.
2 mm	0.107	0.440	9.09	0.590	1.052	1.099	0.204	0.063	0.024	0.003	Bal.
NPM1	0.082	0.465	8.96	0.060	2.950	2.947	0.195	0.053	0.016	0.0076	Bal.
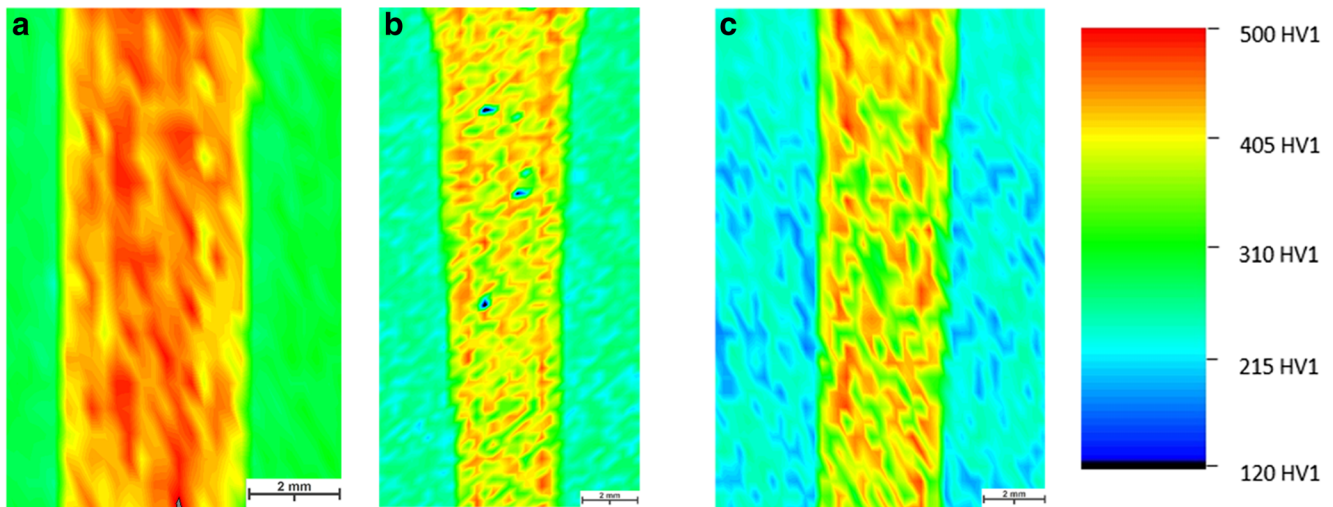
Fig. 7 Hardness distribution of the cross section, all in as-welded condition with corresponding color scale. **a** NPM1 with 2mm P91 interlayer. **b** NPM1 joint weld without filler material. **c** P91 blind weld

The results obtained by the conducted experiments lead to the following conclusions:

- The influence of the alloying elements, especially boron, on the hot cracking behavior was investigated by producing bead on plate welds of the MarBN steel NPM1 and two conventional martensitic 9% Cr creep–resistant steels (P91, P92), which then were compared to each other. NPM1 and P92 both showed hot cracks within the fusion zone, whereas no hot cracks could be found in the cross section of the P91 welds. Therefore, P91 was shown to be the more promising filler material than P92.
- Different approaches were conducted to locally (de-)alloy NPM1 with P91 and a minimum needed dilution of P91 was found.
- Interlayer welds with varying thicknesses (1.5 mm, 2.0 mm, and 2.5 mm) were performed. With the given welding parameter configuration, a 2.0mm interlayer is required to produce macroscopically hot crack-free welds.
- To confirm a homogeneous mixture of the two martensitic Cr steels, EDX investigations were conducted and showed the homogeneity within the fusion zone.
- Additionally, a chemical analysis of the 1.5mm and the 2.0mm interlayer welds as well as a reference weld without filler metal was carried out. Results of the chemical analysis showed that local (de-)alloying worked quite well. In the weld metal of the interlayer welds, less boron was detected than in the reference weld.
- However, within the fusion zone of the interlayer welds, an extremely hard and quite large phase was detected. EBSD and EDX investigations revealed a $M_{23}C_6$ structure.
- Hardness mappings of the interlayer weld showed a higher hardness within the fusion zone (440 HV1) compared to

welds of the two base materials (404 HV1 for NPM1 and 390 HV1 for P91). The reasons for the increase in hardness have to be investigated more in detail.

5 Outlook

Further investigation of the mechanical behavior of the interlayer welds has to be carried out. In particular, the influence of the found phase within the fusion zone on the mechanical properties of the welds would be interesting. Therefore, tensile, impact, and creep tests will be conducted in the as-welded and also in the post weld heattreated condition.

References

1. Renewable Energy Policy Network for the 21st Century (2017) Renewables 2017: global status report. Available: http://www.

ren21.net/wp-content/uploads/2017/06/17-8399_GSR_2017_Full_
Report_0621_Opt.pdf. Accessed 03-Mar-2018

2. Cerjak H (2008) The role of welding in the power generation industry. International Institute of Welding, Paris. Proceedings of the IIW International Conference Safety and Reliability of Welded Components in Energy and Processing Industry, pp 17–27

3. Francis JA, Mazur W, Bhadeshia HKDH (2006) Review type IV cracking in ferritic power plant steels. Mater Sci Technol 22(12): 1387–1395

4. Abe F (2011) Effect of boron on microstructure and creep strength of advanced ferritic power plant steels. Procedia Eng 10:94–99

5. Abe F, Horiuchi T, Taneike M, Sawada K (2004) Stabilization of martensitic microstructure in advanced 9Cr steel during creep at high temperature. Mater Sci Eng A 378(1–2 SPEC. ISS):299–303

6. Schlacher C, Béal C, Sommitsch C, Mitsche S, Mayr P (2015) Creep and damage investigation of advanced martensitic chromium steel weldments for high temperature applications in thermal power plants. Sci Technol Weld Join 20(1):82–90

7. U. Dilthey (2006) Schweißtechnische Fertigungsverfahren 1 Schweiß- und Schneidtechnologien, VDIBuch. Springer-Verlag, Berlin, Heidelberg

8. W glowski MS, Błacha S, Phillips A (2016) Electron beam welding - techniques and trends - review. Vacuum 130:72–92

9. Rabl A, Pixner F, Blatesic D, Béal C, Enzinger N (2018) Influence of the focus wobbling technique on the integrity and the properties of electron beam welded MarBN steel. International Institute of Welding, Paris, IIW Document IX-C-1082-18, Intermediate Meeting, Genova

10. Enzinger N, Loidolt P, Wiednig C, Stuetz M, Sommitsch C (2017) Electron beam welding of thick-walled copper components. Sci Technol Weld Join 22(2):127–132

11. Wang T, Zhang BG, Chen GQ, Feng JC, Tang Q (2010) Electron beam welding of Ti-15-3 titanium alloy to 304 stainless steel with copper interlayer sheet. Trans Nonferrous Met Soc China (English Ed. 20(10):1829–1834

12. Barreda JL, Santamaría F, Azpiroz X, Irisarri AM, Varona JM (2001) Electron beam welded high thickness Ti6Al4V plates using filler metal of similar and different composition to the base plate. Vacuum 62(2–3):143–150

13. Mayr P (2007) Evolution of microstructure and mechanical properties of the heat affected zone in B-containing 9% chromium steels. Weld World 54(July):1–15

14. Abe F (2014) Development of creep-resistant steels and alloys for use in power plants. In Structural Alloys for Power Plants: Operational Challenges and High-Temperature Materials (pp. 250–293). Elsevier Inc. https://doi.org/10.1533/9780857097552.2.250

15. Sabitzer C, Béal C, Enzinger N, Sommitsch C (2016) Microstructure and mechanical properties of MarBN steel electron beam welds. 42nd MPA-Seminar, Stuttgart

16. Austrian Standards: ÖNORM EN 10216-2 (2014) Seamless steel tubes for pressure purposes - Technical delivery conditions - Part 2: Non-alloy and alloy steel tubes with specified elevated temperature properties, Vienna

17. Hasegawa Y (2014) Grade 92 creep-strength-enhanced ferritic steel. In Coal Power Plant Materials and Life Assessment: Developments and Applications (pp. 52–86). Elsevier Inc. https://doi.org/10.1533/9780857097323.1.52

18. Abe F (2008) Precipitate design for creep strengthening of 9% Cr tempered martensitic steel for ultra-supercritical power plants. Sci Technol Adv Mater 9(1):013002

19. Abe F, Tabuchi M, Kondo M, Tsukamoto S (2007) Suppression of type IV fracture and improvement of creep strength of 9Cr steel welded joints by boron addition. Int J Press Vessel Pip 84(1–2):44–52

20. Oñoro J (2006) Martensite microstructure of 9-12%Cr steels weld metals. J Mater Process Technol 180(1–3):137–142

21. Sam S, Das CR, Ramasubbu V, Albert SK, Bhaduri AK, Jayakumar T, Rajendra Kumar E (2014) Delta ferrite in the weld metal of reduced activation ferritic martensitic steel. J Nucl Mater 455(1–3):343–348

22. Schulze G (2010) Die Metallurgie des Schweißens. Springer-Verlag, Berlin